ELSEVIER

International Journal of Heat and Fluid Flow 19 (1998) 23–30

International Journal of HEAT AND FLUID FLOW

Body capturing in impacting supersonic flows

P.S. Cumber [a,*], M. Fairweather [a], S.A.E.G. Falle [b], J.R. Giddings [c]

[a] *BG Technology Gas Research and Technology Centre, Ashby Road, Loughborough, Leicestershire LE11 3GR, UK*
[b] *Department of Applied Mathematics, The University of Leeds, Leeds LS2 9JT, UK*
[c] *Mantis Numerics Ltd., 46 The Calls, Leeds LS2 7EY, UK*

Received 16 November 1996; accepted 4 October 1997

Abstract

A mathematical model of sonic and supersonic flows, validated previously for the prediction of free jets and jets which impinge a flat surface orthogonally, is used to simulate the near field structure of supersonic flows which impact a number of cones. Representation of the impacted surfaces, which are misaligned with the finite-volume grid employed, is by means of a body capturing technique based on the use of hierarchical, adaptive Cartesian grids. The accuracy of the model and the body capturing approach is assessed by comparing predictions with experimental data on impinging supersonic flows available in the literature. For the axisymmetric situations considered, results derived from the model are found to be in close agreement with data on the location of both free and attached shocks formed in the vicinity of the impacted objects, with the model also providing good estimates of pressures occurring on the surface of the cones.

Keywords: Supersonic; Impingement; Cones; Mathematical model; Body capturing; Adaptive grids

Notation

d	nozzle diameter
D	cone diameter
h	nozzle-to-cone apex spacing
k	turbulence kinetic energy
M	Mach number
P	surface pressure
P_a	ambient pressure
P_0	nozzle exit pressure
r	axial co-ordinate
s	distance along solid-surface
z	radial co-ordinate

Greek

Δr	grid spacing in the r direction
Δz	grid spacing in the z direction
ε	dissipation rate of k
ρ	local density
ρ_a	ambient density

1. Introduction

Impacting jet flows are of interest in many engineering applications. Examples include the operation of vertical take-off and landing aircraft, the launch of rockets, and many cooling, heating and drying processes used in industry. Of particular interest in the present work, this flow situation is also encountered in assessments of the consequences of accidental releases of gas on both onshore and offshore installations involving high pressure pipework and gas handling plant. More specifically, predictions of the flow field resulting from an impacting jet are used in order to assess the extent of the hazardous zone which exists around any release, and to identify those locations where the presence of ignition sources may result in the establishment of a stable flame.

As well as being of practical interest the complex flow fields established by impacting jets also provide the opportunity to study many fundamental flow phenomena and, as such, these flows represent important test cases for the development and validation of mathematical models. This is particularly the case for compressible jets, where such phenomena as the interaction of shock waves with solid surfaces and flow separation induced by shear layers can occur.

A great deal of experimental work has been performed on the impaction of compressible jets normal to flat surfaces. Examples include the studies of Donaldson and Snedeker (1971) and of Hunt and co-workers (Gummer and Hunt, 1971; Carling and Hunt, 1974). Other flow configurations have received less attention, although sonic and supersonic jets impinging on hemispheres (Donaldson and Snedeker, 1971) and cones (Jennions and Hunt, 1980) have been considered. Besides these axisymmetric situations, the three-dimensional flows that result from the interaction of compressible jets with wedges (Lamont and Hunt, 1976) and inclined flat plates (Lamont and Hunt, 1980) have also been studied, although the complexity of the flows established has meant that understanding has been slow to develop. Corresponding mathematical modelling work on

* Corresponding author.

0142-727X/98/$19.00
PII: S0142-727X(97)10011-X

impinging sonic and supersonic jets is less common, primarily because of the excessive computational demands associated with predicting such complex flows. Iwamoto (1990) and Mahta et al. (1995) did, however, solve the Euler equations for inviscid, axisymmetric flow in order to predict compressible jets impacting a normal surface, with McGuirk and Page (1989) describing a more sophisticated model based on solutions of the viscous flow equations closed using a standard k-ε turbulence model (Jones and Launder, 1972). The present authors (Cumber et al., 1997) also studied compressible jets impacting a normal surface using a model based on solutions of the viscous flow equations obtained using a second-order accurate, finite-volume integration scheme coupled to an adaptive grid algorithm, with closure of the flow equations being achieved using a compressibility corrected variant of the k-ε turbulence model. The latter study considered a number of configurations where features characteristic of impacting compressible flows were present, such as stagnation bubbles and shock induced boundary layer separation, with good agreement between model predictions and experimental data having been found.

All the mathematical modelling work performed to date, and noted above, has focused on jets impacting normal to flat surfaces. In practice, however, there are many flows of interest where a jet impinges a flat surface obliquely, or impacts objects such as cones, spheres and cylinders which cannot be readily aligned with the computational mesh. The present paper describes the application of the mathematical model outlined by Cumber et al. (1994, 1995, 1997) to predicting the near field regions of supersonic jets which impact a cone, and validates model predictions against experimental data on axisymmetric flows (Jennions and Hunt, 1980). In performing these calculations, use is made of the body capturing technique of Falle and Giddings (1993) in which impacted objects are represented using hierarchical, adaptive Cartesian finite-volume grids. In order to further prove the suitability of the latter technique for predicting such flows, comparison of model predictions and experimental data obtained by Ladenburg et al. (1948) is also made for situations where a supersonic free stream flow impinges on a cone. The work described is an extension of earlier studies by the present authors which validated the mathematical model considered below for application to the prediction of underexpanded free jets (Cumber et al., 1994, 1995) and supersonic jets impacting a flat plate orthogonally (Cumber et al., 1997).

2. Body capturing

In recent years there has been considerable interest in the development and use of adaptive Cartesian grids for computing complex flows, e.g., Berger and Colella (1989) and Falle and Giddings (1993). In contrast to alternative approaches, such as those based on body-fitted grids, adaptive Cartesian grids offer significant savings in grid generation costs and the simpler implementation of numerical algorithms, as well as avoiding the difficulties associated with highly distorted cells that occur when grids are fitted to solids with complicated shapes. In addition, many flow situations of interest to industry, e.g., as encountered in safety assessments of offshore modules, are sufficiently complex to preclude the use of body-fitted grids since their prescription would be excessively time consuming, if indeed possible at all.

The main disadvantage of Cartesian grids is that they do not represent solid surfaces as accurately as body-fitted grids. This advantage may be overcome using a variety of techniques, although the simplest approach is to represent surfaces misaligned with the finite-volume grid using a series of steps in the grid. Grid refinement through adaption then provides an increasingly accurate representation of the surface. The problem then arises that in inviscid flows the steps generate O(1) errors which propagate out into the flow. In viscous flows, however, it is possible to confine these errors to the boundary provided the mesh Reynolds number at the solid surface is sufficiently small. In this sense, therefore, this approach can be regarded as body capturing in that, like shock capturing, O(1) errors are tolerated at the solid surface, although algorithms are employed to ensure that these errors do not propagate into the rest of the computational domain.

Falle and Giddings (1993) evaluated this technique using numerical simulations of the Blasius boundary layer on a flat plate inclined at an angle of 30° to the grid, a supersonic flow past a wedge and a shock incident on a cylinder. Good agreement with the Blasius analytic solution (e.g., Tritton, 1988) was achieved for the boundary layer flow using only 10 control volumes across that layer – comparable to the number of cells required using body-fitted grids. In addition, for the compressible flows considered, predicted shock locations and orientations agreed well with inviscid flow theory and available Schlieren photographs. In the latter flows the stepped cell representation of smooth surfaces generated artificial weak shocks attached to the surfaces. For these inviscid flows, however, viscosity had a negligible influence on the dominant flow features, and was therefore increased above its laminar value in order to dissipate the artificial shocks and prevent errors at the wall from polluting the rest of the solution.

In the present paper the body capturing technique is applied to both inviscid and turbulent, compressible impacting flows. For the inviscid case the ability of this approach to predict flow quantities both remote and close to the impacted surface is investigated, with viscosities again being adjusted in order to prevent errors. Where an impacting flow is both compressible and turbulent, however, the viscosity cannot be treated as a free parameter to use as a false shock dissipation mechanism as the Reynolds number must be preserved. Such flows therefore represent a much more demanding test of the body capturing technique. Despite this, it is demonstrated that the latter technique can be applied successfully to turbulent compressible flows.

3. Mathematical model

In the interests of brevity, only the essential details of the mathematical model employed in the present work are reproduced below. Full details may be found in Cumber et al. (1994, 1995, 1997).

3.1. Governing equations

Predictions for inviscid flows were based on solutions of transport equations for the conservation of mass, momentum and energy, expressed in axisymmetric and steady state form. The system of equations was augmented by the ideal gas law for solution. Turbulent flows were simulated using high Reynolds number versions of the fluid flow equations, again expressing conservation of mass, momentum and energy, with density-weighted (Favre) averaging being used as most appropriate for the variable density flows of interest. Closure of this set of equations was achieved using a two-equation, k-ε turbulence model (Jones and Launder, 1972), modified in line with the recommendations of Sarkar et al. (1991) in order to account for the increase in turbulence energy dissipation rates in compressible flows caused by the formation of compression waves in the instantaneous flow field. Modelling constants employed were standard values found to give acceptable

agreement between theoretical predictions and experimental data in a wide range of flows (Jones and Whitelaw, 1982).

3.2. Computational procedure and boundary conditions

The model described required the solution of a system of coupled partial differential equations. Solutions were obtained by expressing the equation set in cylindrical co-ordinates, and integrating the time dependent form of these equations numerically by time-marching to a steady state.

Integration was achieved using a second-order accurate, finite-volume scheme. Discretization of the descriptive equations therefore followed a conservative, control volume approach, with values of the dependent variables stored at the centres of the computational cells over which the differential equations were integrated. Diffusion and source terms in the modelled equations were approximated using central differencing, whilst approximations to the inviscid (advective and pressure) fluxes were derived using a second-order accurate variant of Godunov's method. The latter method was derived from a conventional first-order Godunov scheme by introducing gradients within computational cells using a non-linear, slope-limiting function which ensures monotinicity. In its fully explicit, time-accurate form the method uses a predictor–corrector procedure where the predictor stage is spatially first-order and is used to provide an intermediate solution at the half-time between time steps. This in turn is used at the corrector stage for the calculation of second-order fluxes.

To increase the rate of convergence a diagonalised implicit scheme was also employed. This scheme first calculates the explicit rate of change to second-order space accuracy, as described above, and then applies diagonalised implicit operators in each of the space directions to make the scheme implicit for sound waves and diffusion. This allows the calculation to proceed using much larger time-steps, based on advection velocities rather than sound waves, than would be possible using the explicit scheme alone. The composite scheme is nominally second-order accurate in space and first-order in time, since steady-state solutions are of interest in the present work the time accuracy of the scheme is unimportant.

An adaptive finite-volume grid algorithm was employed in order to avoid the normally excessive computational cost involved in capturing shock structures. This method used a two-dimensional, rectangular mesh, with local adaption being achieved by overlaying successively refined layers of computational grid. At the start of any calculation, the first two grid layers covered the entire computational domain, with finer grids only being generated in regions which required higher resolution. Local adaption was achieved by generating estimates of the local truncation error for all transported variables by comparing solutions on adjacent grid levels. The grid was then refined if any of these errors exceeded a given tolerance, taken to be 2%. In the results presented below, up to seven levels of grid were used. Further details of the numerical and adaptive grid algorithms may be found in Falle (1991) and Falle and Giddings (1993).

Ladenburg et al. (1948) considered the flow of a supersonic air free stream ($M = 1.7$) over cones with apex angles of 60° and 90°. In simulating these flows the impacted object was located on a line of symmetry, with the cone apex at the origin ($r,z = 0,0$) of the co-ordinate system. The supersonic free stream was imposed at boundaries located at $-z$ and $+r$, with the pressure, density and velocity being prescribed consistent with the hyperbolic nature of the flow. A no-slip boundary was imposed on the surface of the impacted object. At the exit from the computational domain, at $+z$, a free flow boundary condition was prescribed at which external flow quantities were extrapolated from internal values.

In simulating the experiments of Jennions and Hunt (1980) the flow configuration was approximated using a jet issuing from a circular cross-sectioned pipe placed below a right cone. Considering the centre of the pipe exit as ($r,z = 0,0$), the boundary conditions applied in the computations assumed symmetry along the jet centre-line, represented as the z axis at $r = 0$, with a constant pressure entraining boundary being used in regions outside the pipe at $-z$. On the external surface of the pipe and the impacted cones finite-volume solutions were patched onto fully turbulent, local equilibrium wall law profiles. The remaining boundaries, at $+r$ and $+z$, were treated as a constant pressure surface and a free flow boundary, respectively. In performing calculations the sensitivity of computed solutions to the positioning of the free boundaries was investigated, and in the results presented below these surfaces were located at positions which had a negligible influence on the flow. Inlet conditions at the pipe exit were specified as supersonic, with density, pressure and velocity being prescribed. The convergent–divergent nozzle actually used by Jennions and Hunt (1980) produced a weak shock emanating from the nozzle wall downstream of the throat of the nozzle. The mean velocity profile exiting the nozzle was therefore specified in line with predictions of an inviscid model of the nozzle flow made by Jennions (1980). The remaining variables required at the nozzle exit were prescribed to be uniform, except the turbulence kinetic energy and its dissipation rate which were taken from Hinze (1977), consistent with the existence of a boundary layer attached to the nozzle wall.

All the simulations used computational domains which ranged in size depending on the flow geometry, the measured data available for comparison purposes and the sensitivity of computed solutions to the positioning of the free boundaries. For small computational domains, and for regions close to nozzle exits and surfaces, uniform grids were used, whereas for larger domains and regions remote from solid surfaces geometrically expanding grids were employed with a maximum expansion ratio of 1.05. The fineness of numerical grid required to obtain grid independent solutions was examined for each of the flows studied, and in the results presented below a sufficiently large number of computational nodes was used in order to ensure that model solutions were essentially free of numerical error.

Fig. 1 shows a portion of the adapted grid used in simulating one of the impacting flows studied by Jennions and Hunt (1980). The jet considered issued from a convergent–divergent nozzle with an exit diameter, d, of 30 mm at a nominal Mach number of 2.2. The ratio of local nozzle exit pressure to ambient pressure, P_0/P_a, for this release was 2, with the apex of the cone being a distance, h, of one diameter from the exit plane of the nozzle. This particular simulation employed five levels of finite-volume grid, with the two coarsest levels being non-adaptive. As can be seen from this figure, in which the z axis at $r = 0$ is a symmetry boundary, the finest mesh is located adjacent to the impacted surface (at 45° to the co-ordinate system) and the pipe exit (at the centre of the lower boundary), and around shocks and regions of steep local gradients between the pipe exit and the surface. Fig. 2 illustrates the sensitivity of predictions of surface pressure, P, to the grid resolution used in computations of the same jet considered in Fig. 1, but with a nozzle-to-cone apex spacing of $2d$. In this and subsequent figures, s is used to denote distance along a solid surface away from the stagnation point, and Δz and Δr represent the grid spacing used in each of the co-ordinate directions. Results obtained using the two finest meshes are seen to be essentially grid independent.

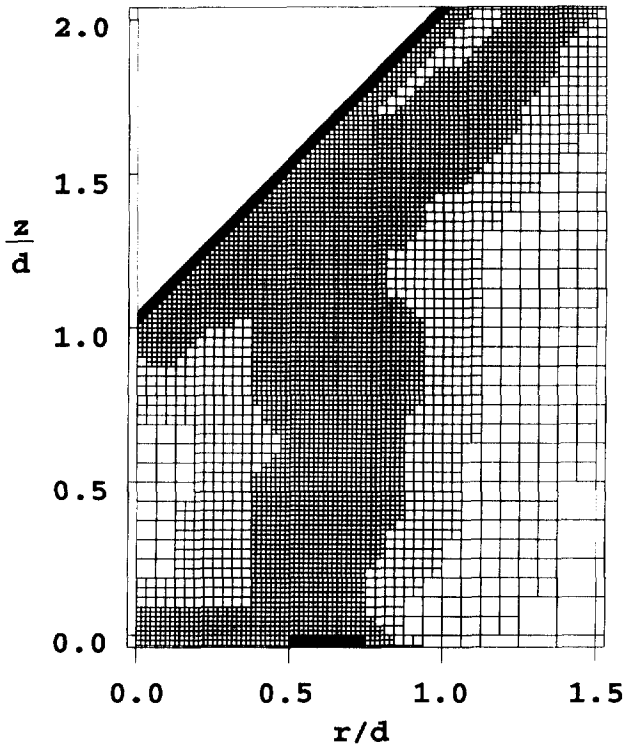

Fig. 1. A portion of the adapted grid used in simulating an impacting jet ($h = 30$ mm).

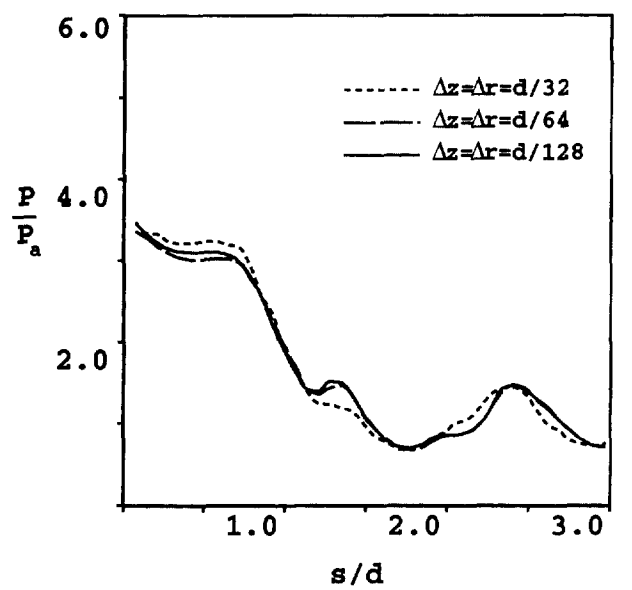

Fig. 2. Effect of grid resolution on predictions of surface pressure for an impacting jet ($h = 60$ mm).

4. Results and discussion

4.1. Inviscid flows

As noted earlier, in inviscid flows the stepped cell representation of smooth surfaces generates artificial weak shocks attached to those surfaces. Similar to Falle and Giddings (1993), the predictions derived in the present work were based on increasing the viscosity above its laminar value in order to dissipate the artificial shocks and prevent errors at the wall from polluting the rest of the solution. Initial results given below were based on a viscosity set to 10^3 times the laminar value. Sensitivity studies demonstrated that the predicted flow fields remote from the impacted surface were unaffected by the surface representation for this level of dissipation, with predictions derived using a viscosity of 500 and 10^3 times the laminar value being essentially equivalent.

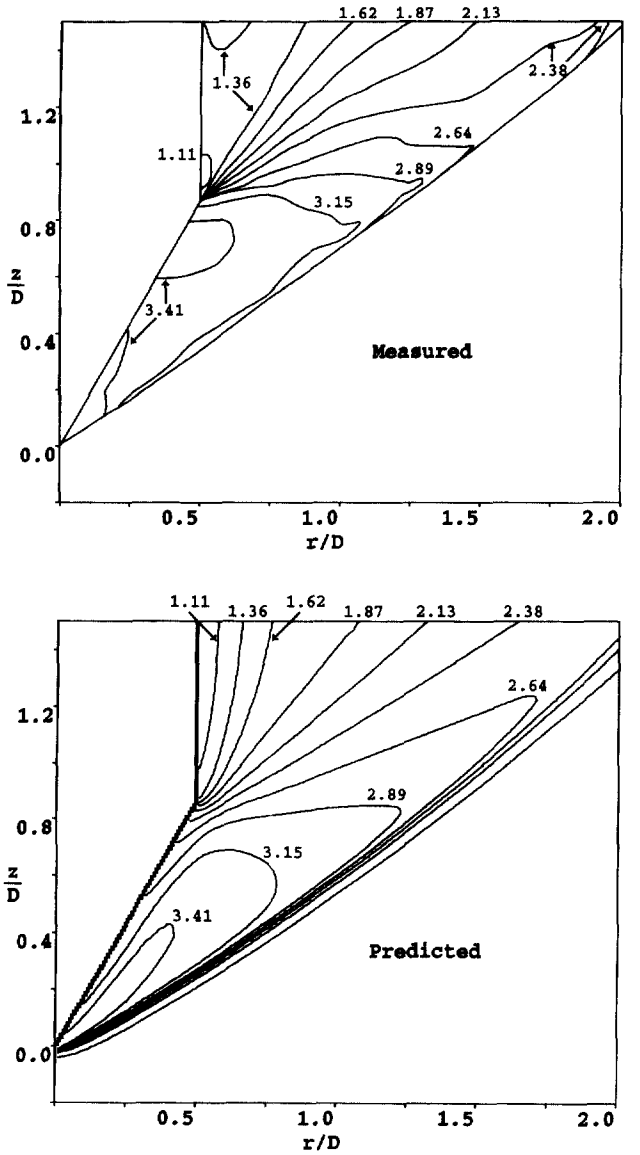

Fig. 3. Density field in the vicinity of a 60° cone impacted by a supersonic air stream.

Ladenburg et al. (1948) used interferometry to study the density field in the vicinity of the cones impacted by the supersonic air stream. Fig. 3 shows measured and predicted density fields for the case where a supersonic stream impacted on a cone with an apex angle of 60°. The results are given in terms of 10, equi-spaced contours which range from $\rho/\rho_a = 1.11$ 3.41. In this and subsequent figures, contour values decrease away from the cone apex. For both the measured and simulated flows a shock is attached to the apex of the cone, with the observed and predicted shock orientation being in close agreement. The predicted shock is, however, smeared relative

to measurements due to the large viscosity used in the computations. Predictions of the density field are in reasonable agreement with observations, with the relatively constant density region just downstream of the cone apex being reproduced. Significant errors do, however, occur in close proximity to the surface within the latter region, and in the wake of the cone, again due to the large value of viscosity employed in the computations.

Similar results are obtained when the cone has an apex angle of 90°, as shown in Fig. 4. Results in this figure are given in terms of eleven, equi-spaced contours which range from $\rho/\rho_a = 1.02$–4.43. For this flow the shock is detached from the apex of the cone, with shock location and orientation being predicted accurately, but with the predicted shock again being smeared. In terms of the density field, the overall level of agreement between theory and experiment is on the whole better than for the 60° case, although problems are still evident with predictions close to the surface of the cone and in its wake.

In view of the relatively poor agreement between predictions of the model and experimental data obtained for these two cases, further simulations were performed in order to investigate the mechanism employed for damping artificial, weak surface shocks. For these simulations the turbulent, high Reynolds number versions of the fluid flow equations were solved, as described earlier. Two further transport equations, for the turbulence kinetic energy and its dissipation rate, were therefore included in the computations, together with appropriate boundary conditions. In particular, at the inlet boundary located at $-z$, low levels of turbulence were prescribed, although predicted mean flow fields were found to be insensitive to the actual values used as any initial turbulence decays exponentially within the free stream flow.

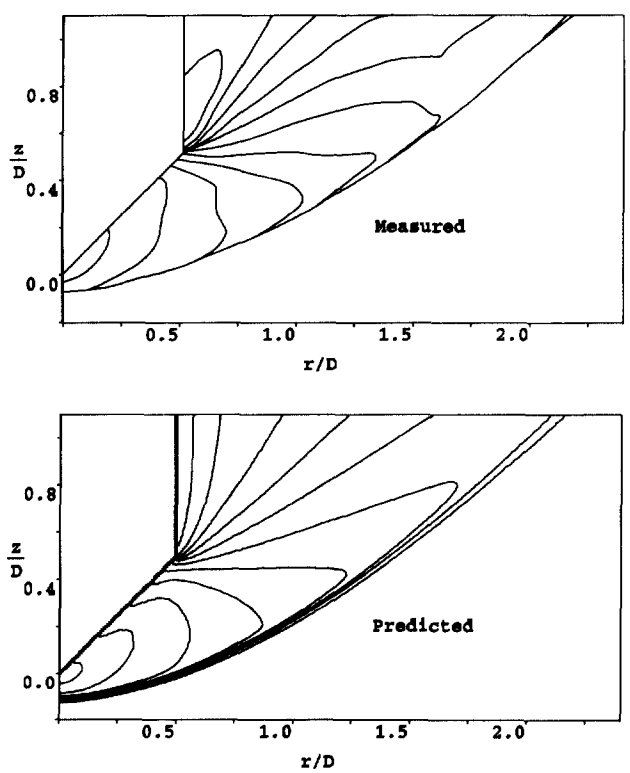

Fig. 4. Density field in the vicinity of a 90° cone impacted by a supersonic air stream.

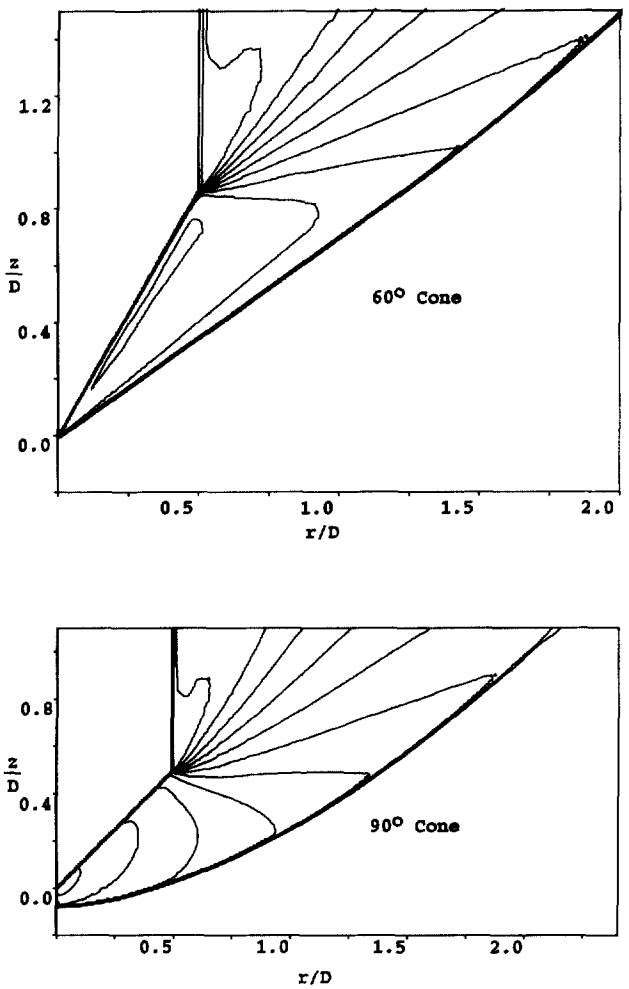

Fig. 5. Predicted density field in the vicinity of the 60° and 90° cones obtained using the turbulence model.

Fig. 5 shows density fields predicted using this approach for both the 60° and 90° cones, with contours used being the same as those employed in Figs. 3 and 4, respectively. The improvement in the predicted density field is seen to be significant, with much sharper shock definition and the correct flow behaviour close to the surface of the cone and in its wake. The improvement in accuracy when using the turbulent, high Reynolds number model is further illustrated in Fig. 6, where measured surface pressures are compared with the inviscid and turbulent predictions. Every aspect of the latter predictions is seen to be in much closer agreement with the pressure distribution measured, particularly in the wake of the cone.

The turbulent model results shown in Figs. 5 and 6 were derived using the laminar viscosity set to its normal value, but with the turbulent eddy viscosity being used as the mechanism for damping false surface shocks. The eddy viscosity is a much more selective tool for damping false shocks than increases in the laminar value since, for the impacting flows considered, its maximum value is naturally located near the impacted surfaces, and tends to increase in response to steep gradients in the velocity field. For these impacting flows, therefore, the artificial shocks generated by the stepped cell representation of the surface are a relativity minor inconvenience since, as the results described above demonstrate, the selective use of a shock damping mechanism, in this case the turbulent eddy viscosity, can be employed to give good agreement between experimental data and model predictions.

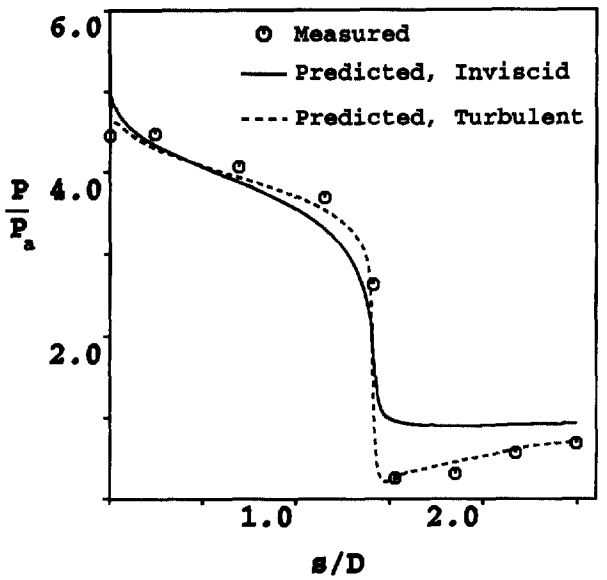

Fig. 6. Pressure distribution on the surface of the 90° cone.

4.2. Turbulent flows

The simulations discussed above illustrate the application of the body capturing technique to compressible inviscid impacting flows. In this section the same technique is applied to the prediction of turbulent compressible jets impacting cones in which the viscosity cannot be treated as a free parameter to use as a false shock dissipation mechanism.

These simulations consider a supersonic underexpanded air jet impacting a cone with an apex angle of 90°, for which experimental data is available from Jennions and Hunt (1980). Two nozzle-to-cone apex separations are examined, but in both cases the jet inlet conditions are identical and as discussed earlier. For both separations ($1d$ and $2d$) it should be noted that the cone apex is significantly upstream of the position where the Mach disc would occur in the free underexpanded jet, measured at $z/d = 2.4$ (Jennions and Hunt, 1980).

Fig. 7 compares predictions of the density field in the vicinity of the cone apex, for the $1d$ separation case, with observed locations of steep density gradients obtained from the shadowgraph of Jennions and Hunt (1980); the latter data indicating the presence of shocks, shear layers and slip-lines. In both the simulation and the experiment the same complex shock structure is seen to exist, with an oblique shock attached to the apex of the cone interacting with the jet shock to form two, three-shock confluence points (indicated by points (a) and (b) in Fig. 7) separated by a portion of normal shock. Both qualitative and quantitative agreement between theory and experiment is good, apart from at the inner three-shock confluence point (point (a)) where the tail shock attached to the cone surface is approximately normal to the cone in the simulation, whereas the observed shock intersects the surface obliquely. The orientation of the observed tail shock relative to the cone surface does, however, suggest that the mean flow would be deflected away from the surface downstream of the shock, although this is not consistent with the observed orientation of the slip-line originating from point (a).

The measured and predicted distribution of pressure on the surface of the cone is compared in Fig. 8. In terms of observed pressures, the initial pressure drop near the apex of the cone is caused by divergence of the flow in this region. This pressure drop is interrupted at $s/d \approx 0.5$ by an increase in pressure caused by the tail shock originating from the inner of the two, three-shock confluence points, with the slight increase in pressure at $s/d \approx 1.6$ being associated with the inner slip-line attaching to the cone. The final region of compression, occurring at $s/d \approx 2.3$, results from both the outer slip-line and the jet boundary impacting on the cone. The model predictions reproduce faithfully all the features of the measured pressure profile, although the increase in pressure associated with the tail shock occurs closer to the apex of the cone than is observed. Again, this finding is inconsistent with the results of Fig. 7 since the observed tail shock intercepts the surface much closer to the apex of the cone than the predicted shock. Computed results near the apex of the cone also underestimate experimental data, and a predicted second shock at $s/d \approx 0.7$, generated as mass

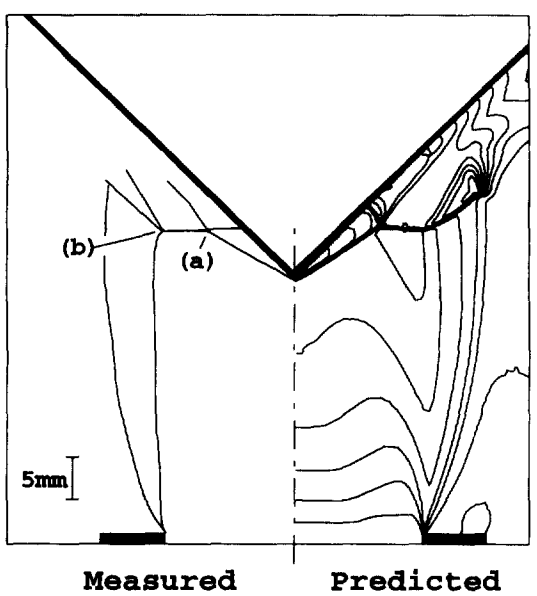

Fig. 7. Shock locations in the impacting jet of Jennions and Hunt ($h = 30$ mm).

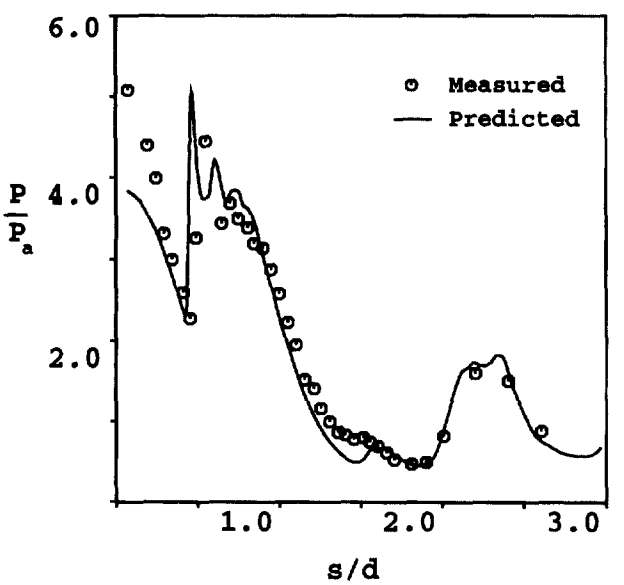

Fig. 8. Pressure distribution on the cone surface for the impacting jet of Jennions and Hunt ($h = 30$ mm).

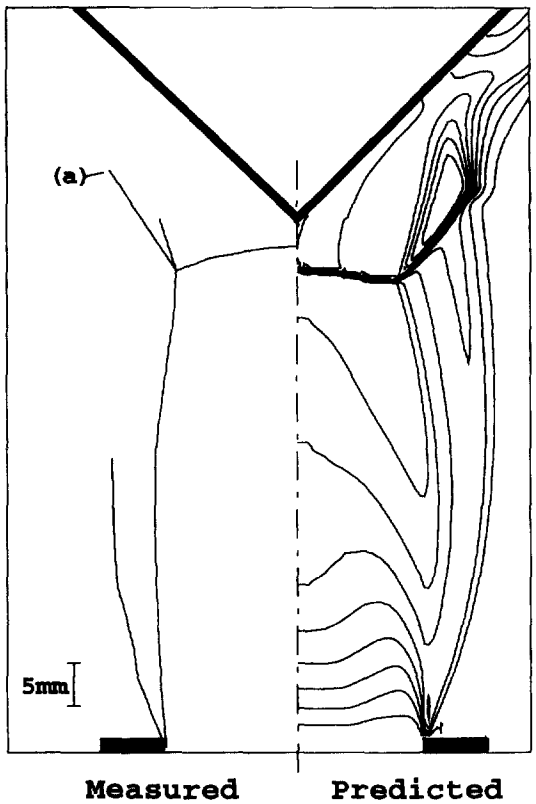

Fig. 9. Shock locations in the impacting jet of Jennions and Hunt ($h = 60$ mm).

accelerating away from the first shock is reflected by the inner slip-line towards the cone surface, is not apparent in the measurements (although this may be due to insufficient resolution in the measurements). Overall, however, the agreement between predictions and measurements is satisfactory.

In the second simulation the nozzle-to-cone apex separation is two nozzle diameters. Fig. 9 again compares predictions of the density field in the vicinity of the cone apex with the observed locations of shocks, slip-lines and shear layers obtained from the shadowgraph of Jennions and Hunt (1980). For this particular nozzle-cone configuration, the main shock occurring close to the cone is detached, and convex towards the cone apex. As in the previous simulation, the predicted density field exhibits all of the features observed in the shadowgraph, although the predicted shock is at an axial distance from the nozzle exit of $z/d \approx 1.8$ compared to an observed value of 1.9. Similar to the previous configuration, the observed and predicted structures can be related directly to the surface pressure measurements shown in Fig. 10. For detached shocks of this type the variation of pressure along the surface of the cone is relatively small, although the shock induced jet expansion (occurring downstream of (a) in Fig. 9) does cause surface pressures to fall relatively rapidly from $s/d \approx 0.7$. The local pressure peak, $s/d \approx 1.2$, is associated with the slip-line originating from the triple point attaching to the cone body, with the final peak at $s/d \approx 2.4$ being caused by the jet boundary impacting on the cone. Good agreement is again obtained between model predictions and data for surface pressure.

5. Conclusions

A mathematical model of sonic and supersonic flows has been used to simulate the near field structure of supersonic flows which impact a number of cones, and its accuracy assessed by comparing predictions with experimental data available in the literature. The body capturing representation of impacted surfaces misaligned with the computational mesh, based on the use of hierarchical adaptive Cartesian grids, has been shown to be capable of giving accurate predictions of flow quantities close to and remote from the surface of objects impacted by both inviscid and turbulent compressible flows.

For the axisymmetric flow situations considered, predictions of the model were found to reproduce faithfully the observed locations of free and attached shocks, and slip-lines and shear layers, formed in the vicinity of cones impacted by a supersonic free stream and a jet. Measurements of pressure occurring on the surface of the cones were also predicted with acceptable accuracy.

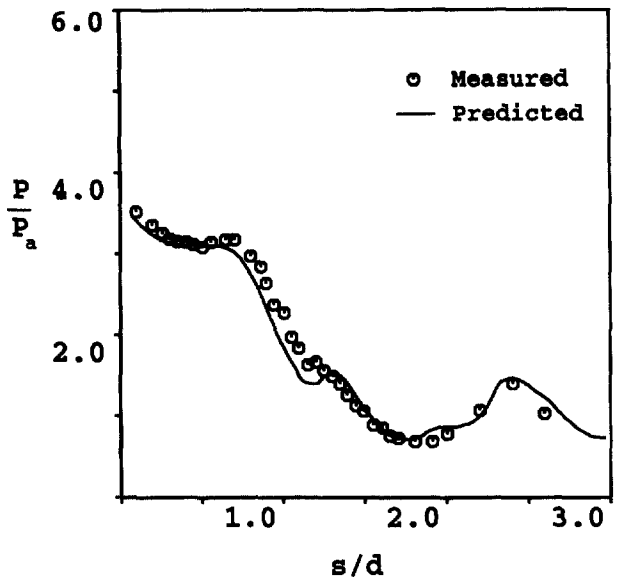

Fig. 10. Pressure distribution on the cone surface for the impacting jet of Jennions and Hunt ($h = 60$ mm).

Acknowledgements

The calculations reported in the paper were made using a modified version of the Mantis Numerics Ltd. code, COBRA. This paper is published by permission of BG Technology.

References

Berger, M.J., Colella, P., 1989. Local adaptive mesh refinement for shock hydrodynamics. J. Comput. Phys. 82, 64–84.

Carling, J.C., Hunt, B.L., 1974. The near wall jet of a normally impinging, uniform axisymmetric, supersonic jet. J. Fluid Mech. 66, 159–176.

Cumber, P.S., Fairweather, M., Falle, S.A.E.G., Giddings, J.R., 1994. Predictions of the structure of turbulent, moderately underexpanded jets. ASME J. Fluids Engrg. 116, 707–713.

Cumber, P.S., Fairweather, M., Falle, S.A.E.G., Giddings, J.R., 1995. Predictions of the structure of turbulent, highly underexpanded jets. ASME J. Fluids Engrg. 117, 599–604.

Cumber, P.S., Fairweather, M., Falle, S.A.E.G., Giddings, J.R., 1997. Predictions of impacting sonic and supersonic jets. ASME J. Fluids Engrg. 119, 83–89.

Donaldson, C. Dup., Snedeker, R.S., 1971. A study of free jet impingement. Part 1. Mean properties of free and impinging jets. J. Fluid Mech. 45, 281–319.

Falle, S.A.E.G., 1991. Self-similar jets. Monthly Notices Roy. Astronom. Soc. 250, 581–596.

Falle, S.A.E.G., Giddings, J.R., 1993. Body capturing using adaptive cartesian grids. In: Baines, M.J., Morton, K.W. (Eds.), Numerical Methods for Fluid Dynamics, Clarendon Press, Oxford.

Gummer, J.H., Hunt, B.L., 1971. The impingement of a uniform, axisymmetric, supersonic jet on a perpendicular flat plate. Aeronautical Quarterly 22, 403–420.

Hinze, J.O., 1977. Turbulence, McGraw-Hill, New York.

Iwamoto, J., 1990. Impingement of under-expanded jets on a flat plate. ASME J. Fluids Engrg. 112, 179–184.

Jennions, I.K., 1980. The impingement of axisymmetric supersonic jets on cones. Ph.D. Thesis, University of London.

Jennions, I.K., Hunt, B.L., 1980. The axisymmetric impingement of supersonic air jets on cones. Aeronautical Quarterly 31, 26–41.

Jones, W.P., Launder, B.E., 1972. The prediction of laminarization with a two-equation model of turbulence. Internat. J. Heat Mass Transfer 15, 301–314.

Jones, W.P., Whitelaw, J.H., 1982. Calculation methods for reacting turbulent flows: A review. Combust. Flame 48, 1–26.

Ladenburg, R., Winckler, J., Van Voorhis, C.C., 1948. Interferometric studies of faster than sound phenomena. Part I. The gas flow around various objects in a free homogeneous supersonic air stream. Phys. Rev. 73, 1359–1377.

Lamont, P.J., Hunt, B.L., 1976. The impingement of underexpanded axisymmetric jets on wedges. J. Fluid Mech. 76, 307–336.

Lamont, P.J., Hunt, B.L., 1980. The impingement of underexpanded axisymmetric jets on perpendicular and inclined flat plates. J. Fluid Mech. 100, 471–511.

Mahta, R.C., Pandya, M.J., Jayachandran, T., 1995. Euler calculations of diffuser flow field, free jets and impinging jets. Internat. J. Numer. Methods Heat Fluid Flow 5, 287–300.

McGuirk, J.J., Page, G.J., 1989. Shock capturing using a pressure-correction method. AIAA Paper 89-0561.

Sarkar, S., Erlebacher, G., Hussaini, M.Y., Kreiss, H.O., 1991. The analysis and modelling of dilatational terms in compressible turbulence. J. Fluid Mech. 227, 473–493.

Tritton, D.J., 1988. Physical Fluid Dynamics, Clarendon Press, Oxford.